A Generalization of RTM Inverse Scattering Imaging Conditions

N. D. Whitmore* (PGS)

SUMMARY

Reverse time migration (RTM) imaging can have significant artifacts which are generated by backscattered and turning waves, where the source and receiver wavefields are in phase. This paper gives a tutorial on an inverse scattering based imaging condition, in which a significant reduction of these artifacts can be achieved. The basic principle has been discussed by others, but we give a simple explanation of the components of the method and then extend it to be more generally applicable to shot, stacks and angle domains. The method is based on an imaging kernel that is the weighted combination of two separate imaging kernels – the time derivative product and the gradient dot product of the source and receiver wavefields respectively. Applications of this method are given for the cases of imaging of single shots, the sum of shots and RTM angle data.

Introduction

Reverse time migration (RTM) is composed of two basic steps – the synthesis of subsurface incident and reflected wavefields and the application of an imaging condition using these two wavefields. In its simplest form, correlation based RTM imaging conditions generate significant low wavenumber artifacts. These artifacts are most often generated by the backscattered and turning waves in the modeling process, which causes the incident and reflected wavefields to be in phase at locations that are not the reflection points. Reduction of these artifacts is often achieved by post processing the image or modifying the imaging conditions to reduce the artifacts in the first place -- or some combination of both.

Post processing methods generally penalize low wavenumber backscattered noise relative to the desired reflection signal (radial wavenumber filters, Laplacians, etc.). However, in recent years there has been an increasing focus on methods that use imaging conditions that use the direction of the propagating wavefields directly in the imaging kernel to reduce the generation of these artifacts during the imaging process (e.g. Zhu, et al. 2009, Stolk, et al. 2009 and others). In this presentation we give a tutorial on one such method, which will be referred to as an inverse scattering imaging condition (ref. C. Stolk, M. Dehoop, T. Op't Root, 2009). As presented in this reference the method is designed to attenuate the backscattered waves using an equally weighted sum of two separate images – one based on the product of the time derivatives of the incident and reflected wavefields and the other based on the dot product of the spatial gradients of the incident and reflected wavefields.

However, due to contributing factors (e.g. complex media, caustics, variable density, elasticity, anisotropy), the inverse scattering condition applied with equally weighted imaging kernels does not produce an optimum reduction in backscattered waves and turning waves. So, the method must be generalized to the case of non-uniform weights. With this generalization, the inverse scattering imaging kernel can be used to improve images when applied to different representations of the data – each time step within a shot, each shot, the summation over shots, and RTM angle gathers or volumes. This paper is a discussion of this generalized inverse scattering condition with examples for both synthetic and real data cases. We also give a tutorial explanation of how the method works.

Method

The most typical forms of RTM correlation noise arise due to scattering from model boundaries and turning waves (see Figure1, showing raypaths and wavefronts from the 2004 velocity BP Benchmark synthetic). If S(**x**,t) and R(**x**,t) are the source and scattered receiver wavefields and A(x) and B(x) are amplitude normalization terms for illumination or angular weighting, then a typical RTM image is computed by an equation of the form:

$$I(\mathbf{x}) = \frac{1}{A(\mathbf{x})}\int B(\mathbf{x})S(\mathbf{x},t)R(\mathbf{x},T-t)dt \qquad (1)$$

A single shot image for the BP benchmark model using this RTM correlation type imaging condition is shown in Figure 2 (with scattered and turning wave raypaths highlighted). The low wavenumber backscattered and turning wave noise exist where the source and receiver wavefields are in phase at locations other than the reflectors and are travelling in the same direction. Far field directions (ray parameters) of these propagating source and receiver wavefields are approximated by:

$$\mathbf{p}_S \cong \frac{\nabla S(\bar{x},t)}{\dfrac{\partial S(\bar{x},t)}{\partial t}} \quad (2a) \qquad \mathbf{p}_R \cong \frac{\nabla R(\bar{x},t)}{\dfrac{\partial R(\bar{x},t)}{\partial t}} \quad (2b) \qquad \cos(\mathbf{p}_S,\mathbf{p}_r) \cong \frac{\mathbf{p}_S \bullet \mathbf{p}_R}{|\mathbf{p}_S||\mathbf{p}_R|} \quad (2c) \qquad |\mathbf{p}_S||\mathbf{p}_R| = \frac{1}{V^2} \quad (2d)$$

The approximate direction angles for the propagating wavefields can also be computed from the ray parameters. Figure 3 shows snapshots for the source and receiver wavefields and the source propagation angles and cosine of opening angle at a single time. Note that the cosine of the opening angle is directly correlated to locations where the wavefields are in phase. Further note that this angular information can be used for binning of angle gathers.

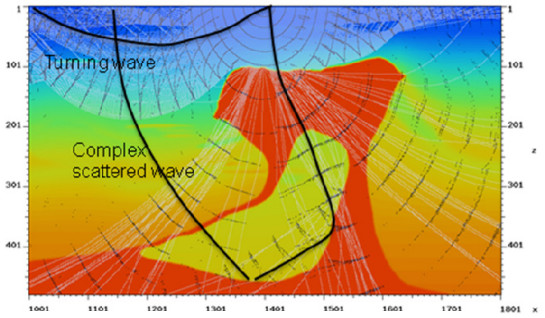

Figure 1 *Raypaths and Wavefronts. Note turning waves and scattered waves.*

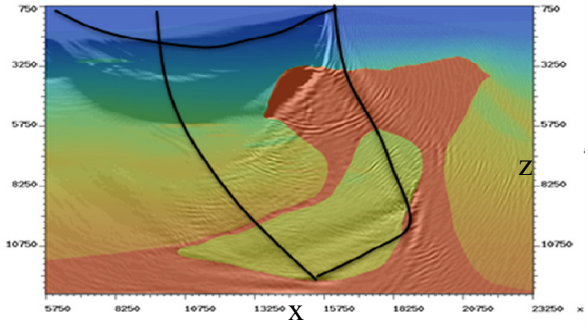

Figure 2 *RTM Correlation Image. Note low wavenumber artifacts.*

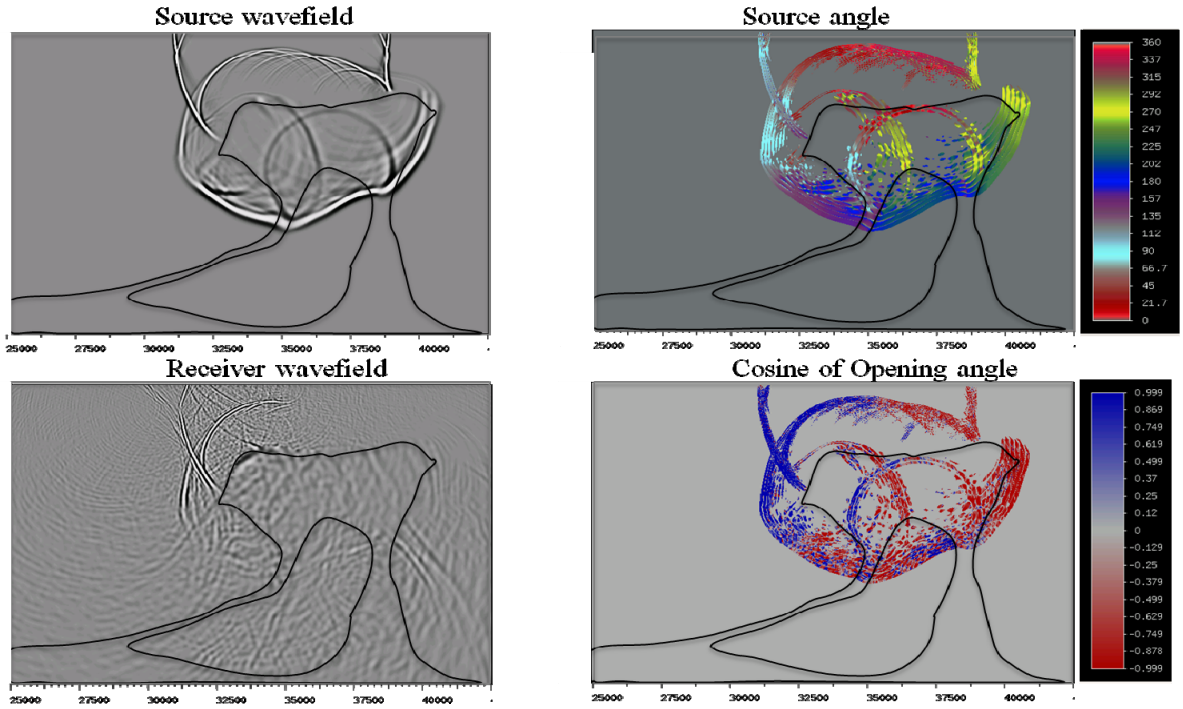

Figure 3 *Wavefield snapshots: Source wavefield, receiver wavefield, source angle (relative to x axis) and cosine of opening angle. Note that the source and receiver wavefields are in phase where the cosine of the opening angle is approximately one (blue color).*

We can use these relationships to investigate the inverse scattering kernel. Consider the case of plane waves in a model with a single velocity contrast with a model reflection coefficient of r_m, as shown in Figure 4. Because the RTM wave propagation generates not only the down-going source field and up-going receiver field, it also generates up-going source and down-going receiver fields. So, there are actually four different combinations of wavefields – as indicated by the ray paths.

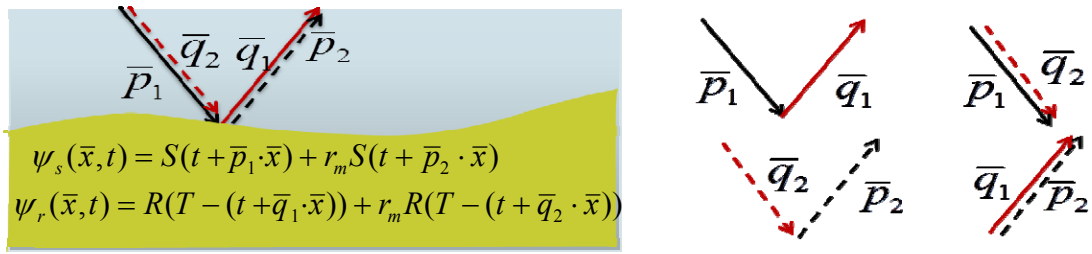

Figure 4 *RTM response of a plane waves in a model with a single velocity transition. Note the 4 combinations of event and that only the* $\bar{p}_1$, $\bar{q}_1$ *combination corresponds to a true reflection.*

At a single time step, consider the imaging kernel made up of the sum of the gradient and time derivative kernels, which for this example results in the following relationship:

$$\nabla\Psi_S(\mathbf{x},t)\bullet\nabla\Psi_R(\mathbf{x},T-t)+\frac{1}{v^2(\mathbf{x})}\frac{\partial\Psi_S(\mathbf{x},t)}{\partial t}\frac{\partial\Psi_R(\mathbf{x},T-t)}{\partial t}=$$

$$\left(\frac{1}{v^2}(\cos(\bar{p}_1,\bar{q}_1)-1)\right)\left(S'(t+\bar{p}_1\cdot\bar{x})R'(T-(t+\bar{q}_1\cdot\bar{x}))\right) \quad \text{<----- True reflection}$$

$$+\left(r_m\left(\frac{1}{v^2}(\cos(\bar{p}_1,\bar{q}_2)-1)\right)\right)\left(S'(t+\bar{p}_1\cdot\bar{x})R'(T-(t+\bar{q}_2\cdot\bar{x}))\right) \quad \text{<----- Backscatter}$$

$$+\left(r_m\left(\frac{1}{v^2}(\cos(\bar{p}_2,\bar{q}_1)-1)\right)\right)\left(S'(t+\bar{p}_2\cdot\bar{x})R'(T-(t+\bar{q}_1\cdot\bar{x}))\right) \quad \text{<----- Backscatter}$$

$$+\left(r_m r_m\left(\frac{1}{v^2}(\cos(\bar{p}_2,\bar{q}_2)-1)\right)\right)\left(S'(t+\bar{p}_2\cdot\bar{x})R'(T-(t+\bar{q}_2\cdot\bar{x}))\right) \quad \text{<---- Model reflection – in phase with the true reflection} \qquad (3)$$

So, for this simple case (no caustics or turning waves and with a plane wave assumption) with equally weighted sums of the imaging kernels, the backscattered terms are annihilated because the rays are collinear and the cosine terms are equal to 1. However, in the general case, an equally weighted sum of these kernels is not sufficient. A more general inverse scattering condition is given in equation (4), where Ψ_S and Ψ_R are the frequency scaled versions of the source S(**x**,t) and R(**x**,t) respectively:

$$I(\mathbf{x})=\frac{1}{2A(\mathbf{x})}\left[\int W_1(\mathbf{x},t)\nabla\Psi_S(\mathbf{x},t)\bullet\nabla\Psi_R(\mathbf{x},T-t)+W_2(\mathbf{x},t)\frac{1}{v^2(\mathbf{x})}\frac{\partial\Psi_S(\mathbf{x},t)}{\partial t}\frac{\partial\Psi_R(\mathbf{x},T-t)}{\partial t}dt\right] \quad (4)$$

$$\Psi_S(x,t)=\frac{1}{2\pi}\int e^{i\omega t}(i\omega)^{-1}[\omega^{-1}\hat{S}(\mathbf{x},\omega)]d\omega \qquad \Psi_R(x,t)=\frac{1}{2\pi}\int e^{i\omega t}[\omega^{-1}\hat{R}(\mathbf{x},\omega)]d\omega$$

With the addition of appropriately computed weights, this general imaging condition attenuates the low wavenumber RTM artifacts occurring in more complex media, including the case of turning waves. In equation (4) the weights are written as both a function of space and time. However, these weights can also be chosen to be constant and equal (equivalent to Stolk, et. al.), a function of space only (to be applied after the sum over shots) or as a function of angles (to be applied to angle volumes or gathers).

Examples

Figure 5 below shows a comparison between standard correlation based imaging conditions versus the general inverse scattering condition applied to a single shot and sum over shots for the BP synthetic.

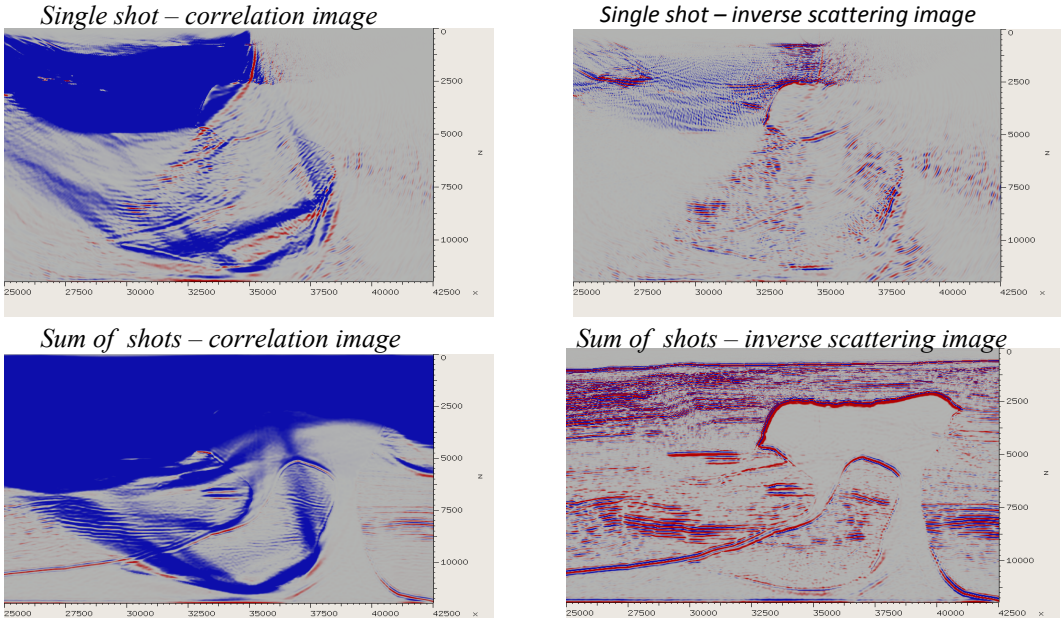

Figure 5 *Single shot and multi-shot RTM images – correlation versus inverse scattering.*

A second example is a real data case from offshore Africa. In this case, angle data for a TTI RTM image was generated using the source field direction vector and dip to map shot data into subsurface angle data. The inverse scattering condition was applied to each angle separately, and then the data was summed over angle. For comparison, the angle gathers and stacks of for the correlation and inverse scattering conditions are shown in Figure 6. Note the reduction in RTM artifacts for both the angle gathers and the final stacks.

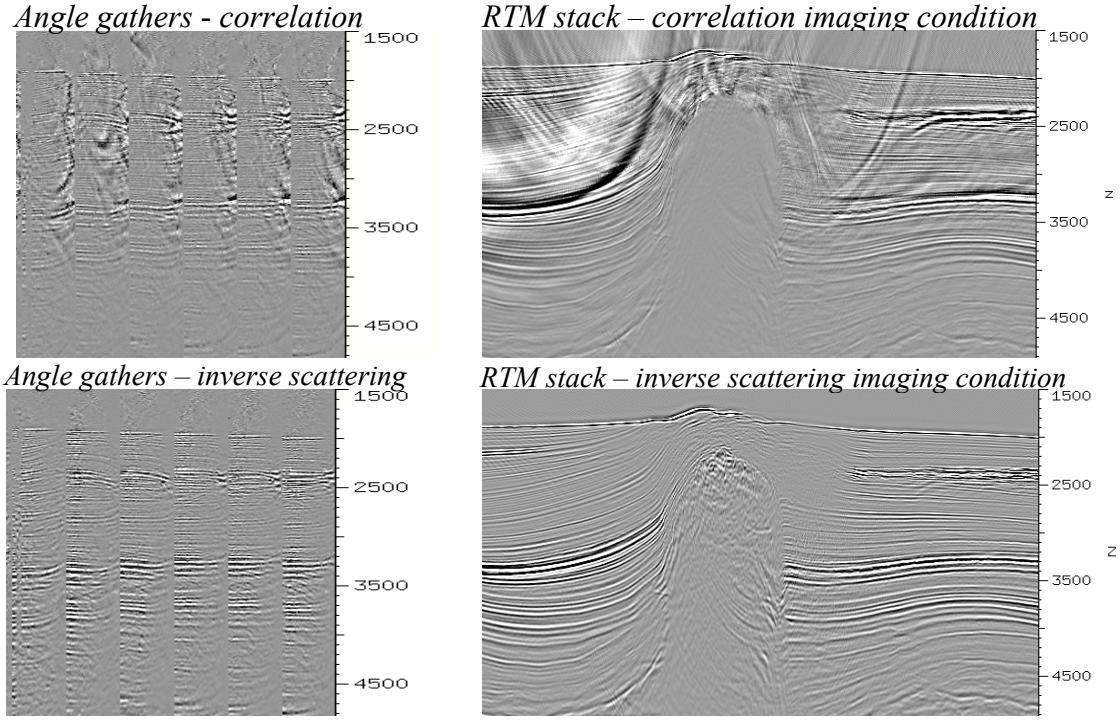

Figure 6 *Angle gathers and stacks for correlation and general inverse scattering imaging conditions.*

Conclusions

This paper gives a tutorial description of an RTM inverse scattering condition that significantly reduces the low wavenumber artifacts over standard correlation based methods. This is achieved by combining time derivative and gradient dot product kernels, but extends previous work by allowing the weights between these kernels to be variable functions of time, space and angle. This allows for greater flexibility in achieving an optimum imaging in several domains – at each time step, for each shot, for each angle or for each stack.

Acknowledgements

We thank PGS for permission to publish present this paper and BP for the BP benchmark synthetic.

References

1. Stolk, C.C., De Hoop, M.V. and Op't Root, T. [2009] Linearized inverse scattering based on seismic Reverse-Time Migration: Proceedings of the Project Review. *Geo-Mathematical Imaging Group (Purdue University, West Lafayette IN)*, **1** (2009), 91-108 and Journal de Mathématiques Pures et Appliquées, 2011.
2. Billette, F. and Brandsberg-Dahl, S. [2005] The 2004 BP velocity benchmark. *67th Annual Conference and Exhibition, EAGE*, Extended Abstracts, B035.
3. Zhu, H., Luo, Y., Nissen-Meyer, T., Morency, C. and Tromp, J. [2009] Elasticimaging and time-lapse migration based upon adjoint methods. *Geophysics*, **74**(6), WCA167-WCA177, doi: 10.1190/1.3261747.